Small-angle neutron scattering study of micellar structures of dimeric surfactants

V. K. Aswal,[1] S. De,[2] P. S. Goyal,[1] S. Bhattacharya,[2] and R. K. Heenan[3]
[1]*Solid State Physics Division, Bhabha Atomic Research Centre, Mumbai 400 085, India*
[2]*Department of Organic Chemistry, Indian Institute of Science, Bangalore 560 012, India*
[3]*ISIS Facility, Rutherford Appleton Laboratory, Chilton, Didcot, Oxon. OX11 0QX, United Kingdom*
(Received 12 June 1997)

Dimeric or gemini surfactants consist of two hydrophobic chains and two hydrophilic head groups covalently connected by a hydrocarbon spacer. Small-angle neutron scattering measurements from bis-cationic $C_{16}H_{33}N^{+}(CH_3)_2$-$(CH_2)_m$-$N^{+}(CH_3)_2C_{16}H_{33}$ $2Br^{-}$ dimeric surfactants, referred to as 16-*m*-16, for different length of hydrocarbon spacers $m=3$–6, 8, 10, and 12, are reported. The measurements have been carried out at various concentrations: $C=2.5$ and 10 mM for all m and $C=30$ and 50 mM for $m \geqslant 5$. It is found that micellar structure depends on the length of the spacer. Micelles are disks for $m=3$, cylindrical for $m=4$, and prolate ellipsoidals for other values of m. These structural results are in agreement with the theoretical predictions based on the packing parameter. It has also been observed that conformation of the spacer and the hydrophobic chains in the interior of the micelle change as the length of the spacer is increased. The concentration dependence for $m \geqslant 5$ shows that the effect of surfactant concentration on the size of the micelle is more pronounced for $m=5$ and 12 than for the intermediate spacers. The fractional charge on the micelle increases with the increase in spacer length and decreases when the concentration is increased [S1063-651X(97)11312-5]

PACS number(s): 61.12.Ex, 61.25.Hq, 82.70.Dd

I. INTRODUCTION

Surfactant molecules [e.g., cetyltrimethylammonium bromide (CTAB)] consist of a hydrophilic head group and a hydrophobic chain connected to the head group. These molecules in aqueous solution above a critical micellar concentration (CMC) aggregate to form micelles. The aggregates formed are of various types, shapes, and sizes, such as globular micelles, cylindrical micelles, and spherical vesicles. The characteristics of these aggregates are determined by the molecular structure of the surfactant molecule as well as by the solution conditions, such as concentration, temperature, and ionic strength [1,2]. Recently, a different class of surfactants has been introduced [3,4]. These surfactants, called dimeric or gemini surfactants, consist of two hydrophobic chains and two hydrophilic head groups covalently attached by a hydrocarbon spacer. Dimeric surfactants have the general formula $C_nH_{2n+1}N^{+}(CH_3)_2$-$(CH_2)_m-N^{+}(CH_3)_2C_nH_{2n+1}2Br^{-}$ and are referred to as *n*-*m*-*n* surfactants. These surfactants possess unusal properties. In particular, they form micelles at very low CMC and are highly efficient in lowering the oil-water interfacial tension in comparison to the single chain counterparts. These properties suggest that the dimeric surfactants are possible candidates for the next generation of surfactants [5]. This paper deals with micellization of dimeric surfactants as studied by small-angle neutron scattering.

Dimeric surfactants are of interest as they provide a system where aggregation behavior can be controlled by varying the spacer while keeping the length of the tail fixed [6]. Israelachvili *et al.* have shown that the type of structure of the self-assembly formed by different surfactants depends upon the geometrical packing parameter (see Sec. IV C) [7]. In dimeric surfactants, the geometrical packing parameter can be varied by varying the length and the conformation of the spacer. For example, when the spacer is shorter than the equilibrium distance between the charged head groups, the spacer remains fully extended to minimize the repulsion between the head groups. This gives rise to a higher value of the packing parameter. In the case where the spacer is longer than the equilibrium distance between the charged head groups the spacer will avoid being in a fully extended conformation. Due to the hydrophobic character of the spacer chain, the same will try to minimize its contact with water by folding inside the micellar interior. This is possible only when the flexibility of the spacer chain is adequate. Thus molecular features, such as the spacer's length and flexibility, are essential for determining the overall shape of aggregates of dimeric surfactants [8].

The micellization behavior of dimeric surfactants has been the subject of several recent publications [8–11]. Cryo-TEM measurements have been reported from the micellar solutions of some of the dimeric surfactants [9]. Depending on the chain and spacer lengths, various types of aggregates, such as ellipsoidal micelles, cylindrical or threadlike micelles, membranes, and vesicles, have been observed. For example, for $n=12$, the micelles are threadlike for short spacers ($m=2,3$), ellipsoidal or spherical for medium chain length spacers ($m=5$–12), and again threadlike or vesicles for long spacers ($m>14$). It was seen that the aggregate structure depends both on the spacer length and on the length of the hydrophobic chains. However, the details of the micellar architecture, such as aggregation number, charge on the micelle, or information about the packing of the surfactant molecules in the micelles, are not obtainable from Cryo-TEM measurements.

Small-angle neutron scattering (SANS) is an ideal technique to study the micellar structures of surfactants. It has been used extensively to understand the micellar structures of various single-chain surfactants [12,13]. Among the dimeric surfactants, only 10-*m*-10 dimeric micellar systems have been studied for different spacers, $m=2$–4 and 6, using

SANS [10]. It has been reported that micelles are ellipsoidal for $m=2$ and slightly elongated spheres for other values of m. In the analysis of the above data, authors have assumed that the spacer resides on the surface of the micelle and hydrophobic chains are fully extended in the interior of the micelle. It is not clear if these approximations are valid. We have reported preliminary SANS measurements from micellar solutions of 16-m-16 dimeric surfactants for different length of spacers [11]. The mixed micelles of 16-m-16 with single-chain surfactant CTAB have also been examined by us [14]. These studies clearly showed that the micellar structure is quite sensitive to the length of the spacer. These experiments were, however, carried out at CIRUS Reactor, Trombay [15], where there were several limitations. Because of the low count rate of the instrument, the measurements were confined to high surfactant concentrations. Under these conditions, additional complications due to interparticle interference effects arise in the data analysis. Moreover, the lowest accessible Q in the Trombay instrument is 0.02 Å^{-1} and hence large micelles (especially $m=3$ and 4) could not be studied. In view of the above, we have now carried out detailed measurements on 16-m-16 dimeric surfactants for $m=3$–6, 8, 10, and 12 using a state-of-the-art low Q (LOQ) diffractometer at ISIS, United Kingdom. The measurements have been extended to quite dilute solutions and the effects of surfactant concentrations on micellar sizes and shapes are also examined.

II. EXPERIMENT

All the dimeric surfactants 16-m-16, $m=3$–6, 8, 10, and 12, were prepared and characterized as described in the earlier paper [11]. The micellar solutions were prepared by dissolving known amount of surfactants in D_2O. The lower concentration of solutions were made by dilution method. The use of D_2O instead of H_2O provides better contrast in neutron experiments. SANS experiments were performed using the LOQ diffractometer at the pulsed neutron source ISIS [16]. LOQ diffractometer uses neutrons of wavelength 2.2–10 Å, simultaneously by time of flight, with a 64×64 cm^2 detector at a distance of 4.1 m from the sample. The measurements were made on the surfactant concentrations $C=2.5$ and 10 mM for all m. For $m\geqslant5$, measurements were also made at $C=30$ and 50 mM. The samples were held in quartz sample holder of thickness 2 mm. The temperature for all the samples was kept at 30 °C. The data were recorded in the Q range 0.009–0.24 Å^{-1}. The measured SANS distributions ($d\Sigma/d\Omega$ vs Q) after standard corrections and normalizations are shown in Figs. 1–7.

III. SANS ANALYSIS

The coherent differential scattering cross section ($d\Sigma/d\Omega$) for a system of monodisperse interacting micelles can be expressed as [17]

$$\frac{d\Sigma}{d\Omega}=n(\rho_m-\rho_s)^2V^2\{\langle F^2(Q)\rangle+\langle F(Q)\rangle^2[S(Q)-1]\}+B. \tag{1}$$

The same expression for noninteracting micelles [i.e., $S(Q)\sim1$] is given by

$$\frac{d\Sigma}{d\Omega}=n(\rho_m-\rho_s)^2V^2\langle F^2(Q)\rangle+B, \tag{2}$$

where n denotes the number density of the micelles, ρ_m and ρ_s are, respectively, the scattering length densities of the micelle and the solvent, and V is the volume of the micelle. The aggregation number N of the micelle is related to the micellar volume V by the relation $V=Nv$, where v is the volume of the surfactant monomer. The volume of the 16-m-16 monomer including the head group is calculated by $v=(1052+26.9m)$ Å^3, as obtained from Tanford's formula [18]. It is different from the way that has been been reported in the earlier paper [11], where the volume of the surfactant monomer was kept as a parameter and determined from the analysis. The same procedure is not used now as it was seen that micellar parameters are not very sensitive to the volume of the monomer.

$F(Q)$ is the single-particle form factor and $S(Q)$ is the interparticle structure factor. B is a constant term that represents the incoherent scattering background, which is mainly due to hydrogen in the sample. For an ellipsoidal micelle

$$\langle F^2(Q)\rangle=\int_0^1[F(Q,\mu)]^2d\mu, \tag{3}$$

$$\langle F(Q)\rangle^2=\left[\int_0^1F(Q,\mu)d\mu\right]^2, \tag{4}$$

$$F(Q,\mu)=\frac{3(\sin x-x\cos x)}{x^3}, \tag{5}$$

$$x=Q[a^2\mu^2+b^2(1-\mu^2)]^{1/2}, \tag{6}$$

where a and b are, respectively, the semimajor and semiminor axes of the ellipsoidal micelle. μ is the cosine of the angle between the directions of a and the wave-vector transfer Q.

For a cylindrical micelle of length $L=2l$ and radius R [19]

$$\langle F^2(Q)\rangle=\int_0^{\pi/2}\frac{\sin^2(Ql\cos\beta)}{q^2l^2\cos^2\beta}\frac{4J_1^2(QR\sin\beta)}{q^2R^2\sin^2\beta}\sin\beta\,d\beta, \tag{7}$$

where β is the angle between the axis of the cylinder and bisectrix. J_1 is the Bessel function of order unity. The disk is a special case of the cylinder when $L\ll R$.

$S(Q)$ specifies the correlation between the centers of different micelles and is the Fourier transform of the radial distribution function $g(r)$ for the mass centers of the micelle. In the analysis for ellipsoidal micelles, $S(Q)$ has been calculated using the mean spherical approximation as developed by Hayter and Penfold [20,21]. In this approximation the micelle is assumed to be a rigid equivalent sphere of diameter $\sigma=2(ab^2)^{1/3}$ interacting through a screened Coulomb potential, which is given by

$$u(r)=u_0\frac{\sigma}{r}\exp[-\kappa(r-\sigma)],\quad r>\sigma, \tag{8}$$

where κ is the Debye-Hückel inverse screening length (which depends on the CMC and the fractional charge on the micelle) and u_0 is the contact potential. The fractional charge $\alpha(=z/N$, where z is the micellar charge) is an additional parameter in the calculation of $S(Q)$. In the case where the intermicellar interactions are not significant in the solutions, $S(Q)\sim 1$.

In general, micellar solutions of ionic surfactants show a correlation peak in the SANS distribution [17]. The peak arises because of the corresponding peak in the interparticle structure factor $S(Q)$ and indicates the presence of electrostatic interactions between the micelles. The peak position in the distribution occurs at $Q_m\sim 2\pi/d$, where d is the average distance between the micelles. The data are well fitted by a Hayter-Penfold–type analysis. The analysis is applicable to the spherical micelles and has also been successfully applied to the ellipsoidal micelles when the axial ratio (a/b) is not very much larger than unity [22,23]. The data analysis procedure to calculate $S(Q)$ for cylindrical or disk micelles, however, has not been developed yet. One of the best ways to analyze data then is to carry out experiments at low concentrations, when $S(Q)\sim 1$. To confirm the above, i.e., $S(Q)\sim 1$, the consistency of analysis is checked by diluting the solution and analyzing the data obtained from such a solution. In the low-concentration measurements, where SANS distributions do not show correlation peak, data have been analyzed assuming $S(Q)\sim 1$. In the case where the distribution shows a peak and the micelles are ellipsoidal, data have been analyzed by taking $S(Q)$ into account as discussed above. In particular, for large aggregates, micelles are known to form polydisperse systems. However, we have assumed them to be monodisperse for the simplicity of the calculation and to limit the number of unknown parameters in the analysis. The dimensions of the micelle, aggregation number, and fractional charge have been determined from the analysis.

IV. RESULTS AND DISCUSSION

A. Effect of spacer length on the micellar structure

To understand the effect of the spacer chain length on the micellar structure, SANS experiments have been carried out on 16-m-16 dimeric surfactants for different lengths, $m=3$–6, 8, 10, and 12, of hydrocarbon spacers. The measurements were made at two concentrations: $C=2.5$ and 10 mM. SANS distributions for $m=3$ do not show a correlation peak at either of the two concentrations. The same is the case for $m=4$ at $C=2.5$ mM. In the case of $C=10$ mM for $m=4$, a peak is shown at $Q_m\sim 0.013$ Å^{-1}. These observations suggest that intermicellar interactions are not very significant in the micellar solutions of $m=3$ and 4 for the above concentrations. It is interesting to note that $d\Sigma/d\Omega$ varies as $1/Q^2$ for $m=3$ in the Q range 0.009–0.07 Å^{-1} and as $1/Q$ for $m=4$ in the Q range 0.009–0.04 Å^{-1}. This has been shown in Figs. 1 and 2, respectively. This suggests that micelles are disks for $m=3$ and cylindrical for $m=4$ [19,24]. The data have been fitted assuming $S(Q)=1$. In the case of $C=10$ mM for $m=4$ system, which shows a peak in the SANS distribution at $Q_m\sim 0.013$ Å^{-1}, data have been analyzed by the same method, i.e., $S(Q)=1$, but fitting the data

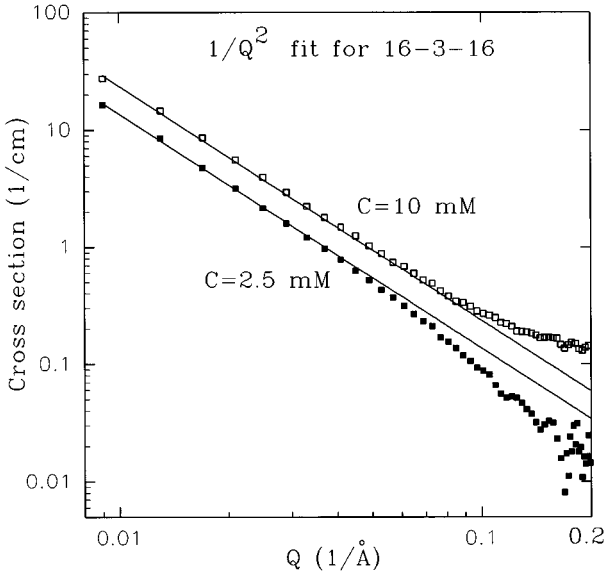

FIG. 1. A log-log plot of SANS distributions for 16-3-16 micellar systems at concentrations of $C=2.5$ and 10 mM. The cross section $d\Sigma/d\Omega$ varies as $1/Q^2$ for $0.009 < Q < 0.07$ Å^{-1}.

in the Q range $Q>2Q_m$. The dimensions of the micelles were obtained by combining Eqs. (2) and (7). The results are given in Table I. Figure 3 shows a comparison between the calculated curves and the experimental data for $C=10$ mM solutions. For 16-4-16, the calculated curve in the low-Q region is from the extrapolation to the fit. The disagreement at low Q for $m=4$ is a reflection of neglecting interparticle correlations.

In Table I we see that in 16-3-16 solutions, micelles are disks with radius $R\sim 200$ Å and thickness $L=27$ Å. Usually, the thickness of a disk or a membrane should be twice the length of a molecule. It is interesting to note that this does not happen for the 16-3-16 dimeric surfactant. When the

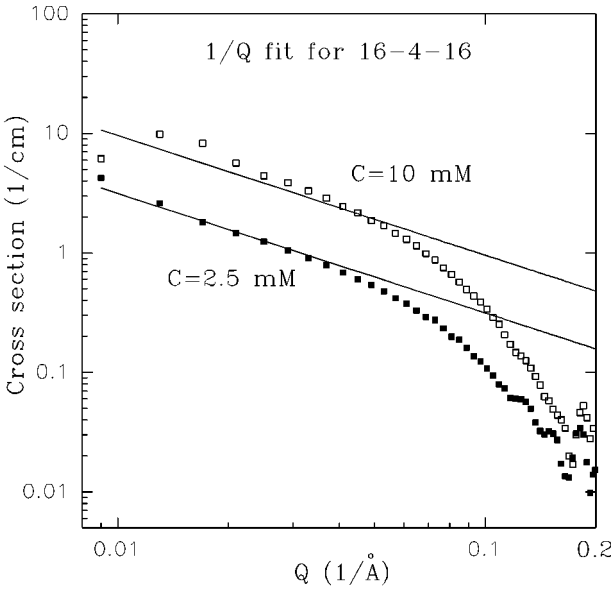

FIG. 2. A log-log plot of SANS distributions for 16-4-16 micellar systems at concentrations of $C=2.5$ and 10 mM. The cross section $d\Sigma/d\Omega$ varies as $1/Q$ for $0.009 < Q < 0.04$ Å^{-1}.

TABLE I. Micellar structures of short spacer 16-*m*-16 dimeric surfactants. (a) 16-*m*-16 ($m=3,4$) micellar systems for $C=2.5$ mM. The parameters have been obtained assuming $S(Q)=1$. (b) 16-*m*-16 ($m=3,4$) micellar systems for $C=10$ mM. The parameters have been obtained assuming $S(Q)=1$. For $m=4$, which shows a correlation peak at $Q=0.013$ Å^{-1}, data have been fitted for $Q>0.025$ Å^{-1}.

System	Structure	Radius R (Å)	Length L (Å)
	(a)		
16-3-16	disk	200.0	27.0
16-4-16	cylinder	25.0	500.0
	(b)		
16-3-16	disk	200.0	27.0
16-4-16	cylinder	25.0	550.0

spacer is short, the two tails of the surfactant molecule come very close to each other. It seems, in that case, that by balancing the intramolecular hydrophobic interaction against the intermolecular hydrophobic interaction, the micelles formed are compact such that head groups alternately pack in up and down directions. That is, the head group of one surfactant molecule faces the tail end of its neighboring molecule. Thus the thickness of the disk is equal to the length of the molecule. For 16-4-16 at $C=2.5$ mM, micelles are cylindrical with length $L\sim500$ Å and radius $R=25$ Å. The value of micellar length for $C=10$ mM data was obtained by assuming that the length is greater than 500 Å and the fitted value came to be 550 Å. It is clear that this number has a large error. It may be mentioned that because of the finite interparticle interaction and limited-Q range, it is not possible to obtain the effect of concentration on the micellar length from the present data. The structural information obtained is similar to the Cryo-TEM measurements, which

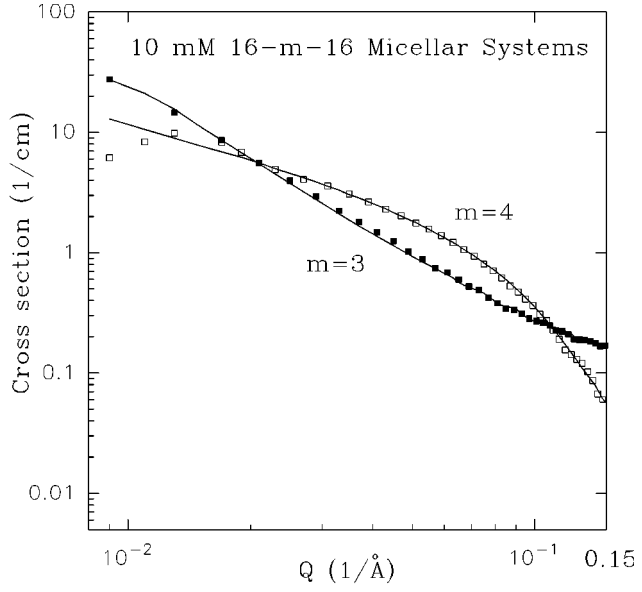

FIG. 3. SANS distributions from 10-mM 16-*m*-16 ($m=3,4$) micellar systems. Solid lines are theoretical fits, where interparticle interference effects have been neglected. For $m=4$, data have been fitted for $Q>0.025$ Å^{-1} .

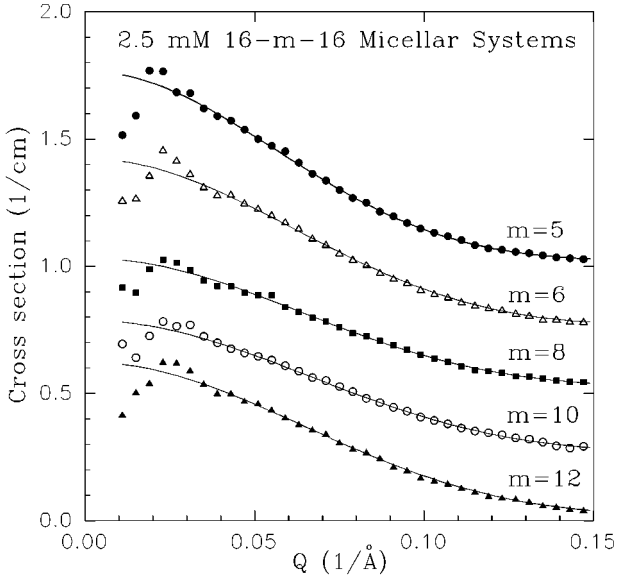

FIG. 4. SANS distributions from 2.5-mM 16-*m*-16 ($m\geqslant5$) micellar systems. Solid lines are theoretical fits without invoking interparticle correlations. The data have been fitted assuming $S(Q)=1$ for $Q>0.04$ Å^{-1}. The solid lines in the low-Q region are extrapolated from the fits. The distributions for $m=5$, 6, 8, and 10 are shifted vertically by 1.0, 0.75, 0.50, and 0.25 units, respectively.

showed that the micelles are threadlike for $m=4$ and vesicles or membranes for $m=3$ [9]. This is consistent with the fact that on the length scale that the SANS technique can probe, the above structures will appear as cylindrical and disks, respectively [25].

The SANS distributions for $m\geqslant5$ at the concentration $C=2.5$ mM are shown in Fig. 4. The shapes of all distributions are similar and there is a correlation peak at about $Q_m\sim0.025$ Å^{-1}. The intensity ($d\Sigma/d\Omega$) of the distributions at the peak position is less than 0.75 cm^{-1}. The slow decrease in intensity with Q suggests that micellar dimensions in these systems are much smaller than those for $m=3$ and 4. It was seen that a Hayter-Penfold–type analysis does not fit the SANS distributions and no meaningful parameters can be extracted. This may be related to the fact that the intensity is very low and there are not enough data points below the peak positions in these distributions. Thus we fitted the distribution for $Q\gtrsim2Q_m$ only, assuming $S(Q)=1$. This showed that micelles are prolate ellipsoidal in these systems. Various parameters obtained from the analysis are given in Table II(a). The aggregation number and the minor axis of the micelle decrease as the length of the spacer increases. The major axis decreases and there is a reverse trend for $m>10$. The effective head group area of surfactant molecules in the micelles has also been determined. It is seen that the effective head group area increases with the length of the spacer and tends to saturate for long spacers ($m>8$). A similar variation of surface area per surfactant at the air-solution interface has also been reported by the surface tension studies on 12-*m*-12 surfactants [26].

The SANS distributions at $C=10$ mM for $m\geqslant5$ are shown in Fig. 5. These distributions show a well-defined peak at about $Q_m\sim0.035$ Å^{-1}. This is because, as the surfactant concentration increases, the distance between the mi-

TABLE II. Micellar structures of 16-m-16 ($m \geq 5$) dimeric surfactants. (a) 16-m-16 ($m \geq 5$) micellar systems for $C = 2.5$ mM. SANS distributions show a correlation peak at about $Q \sim 0.025$ Å^{-1}. The parameters have been obtained assuming $S(Q) = 1$ for $Q > 0.04$ Å^{-1}. Micelles are assumed to be prolate ellipsoidal ($b = c \neq a$). (b) 16-m-16 ($m \geq 5$) micellar systems for $C = 10$ mM. Unlike (a), where $S(Q)$ was neglected, the present parameters have been obtained by a Hayter-Penfold–type analysis, which assumes screened Coulomb potential between the micelles. Micelles are assumed to be prolate ellipsoidal ($b = c \neq a$). The fractional charge on the micelle is the additional parameter in the analysis.

System	Aggregation number N	Minor axis $b = c$ (Å)	Major axis a (Å)	a/b	Effective head group area A (Å^2)
			(a)		
16-5-16	74	24.2	35.6	1.47	128.5
16-6-16	61	23.4	32.0	1.37	138.0
16-8-16	50	22.8	29.2	1.28	154.0
16-10-16	44	22.3	28.0	1.26	165.0
16-12-16	44	21.8	30.6	1.40	170.5

System	Aggregation number N	Fractional charge α	Minor axis $b = c$ (Å)	Major axis a (Å)	a/b	Effective head group area A (Å^2)
			(b)			
16-5-16	79	0.23	24.2	38.0	1.57	124.5
16-6-16	67	0.25	23.4	35.4	1.52	135.0
16-8-16	57	0.27	22.8	33.0	1.45	147.0
16-10-16	50	0.34	22.3	31.8	1.43	161.0
16-12-16	49	0.36	21.8	34.1	1.56	162.0

celles decreases and the peak position in the SANS distribution shifts to a higher-Q value in comparison to that for the $C = 2.5$ mM system. The data have been fitted by the Hayter-Penfold–type analysis. The micellar parameters obtained by this analysis are given in Table II(b). The fractional charge on the micelle as obtained from this analysis is also given in Table II(b). The trends for aggregation number, effective head group area, and minor and major axes are similar as those found for $C = 2.5$ mM solutions [Table II(a)]. The small changes in parameters are connected with the effect of concentration. The fractional charge on the micelle increases as the length of the spacer increases. It is also seen that effective micellar charge ($z = N\alpha$) is nearly proportional to the equivalent sphere radius [$R = (a^2 b)^{1/3}$], consistent with the predictions of the charge renormalization models for globular micelles [27].

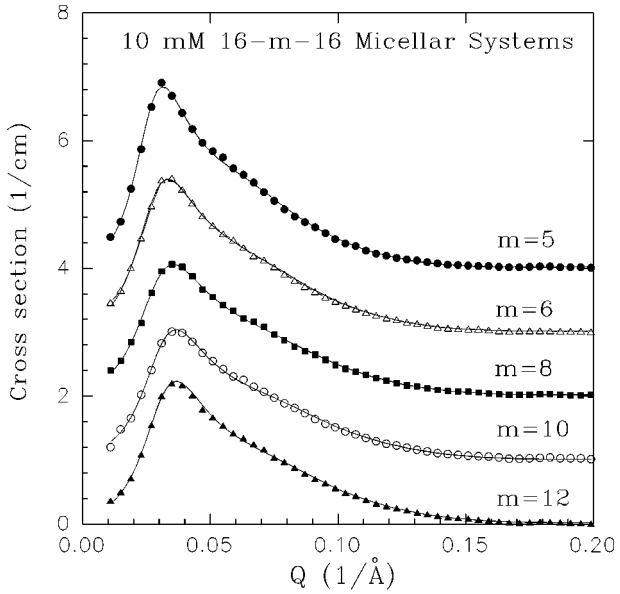

FIG. 5. SANS distributions from 10-mM 16-m-16 ($m \geq 5$) micellar systems. Solid lines are theoretical fits, where interparticle correlations are accounted for using a Hayter-Penfold–type analysis. The distributions for $m = 5$, 6, 8, and 10 are shifted vertically by 4, 3, 2, and 1 units, respectively.

B. Effect of concentration

The results of SANS measurements for $C = 2.5$ and 10 mM have been discussed above. Measurements were made on additional concentrations of $C = 30$ and 50 mM for $m \geq 5$. The SANS distributions are shown in Figs. 6 and 7. SANS patterns for $C = 50$ mM are in good agreement with those reported earlier [11]. Measurements could not be made for high concentrations of $m = 3$ and 4, as they show viscoelastic behavior [28], and the dimensions of micelles in these solutions are expected to be much larger than those that can be measured by SANS.

The peak in the SANS distributions for $C = 30$ and 50 mM is due to the strong electrostatic repulsion between the micelles. Figures 5 and 6 show that for both concentrations the peak intensity and the peak position of the distributions change when the spacer changes. The intensity drops and the peak shifts to higher Q with an increase in the spacer length and the trend changes for $m = 12$.

The above data were analyzed using the method of Hayter and Penfold. Results are given in Table III. It is seen that the

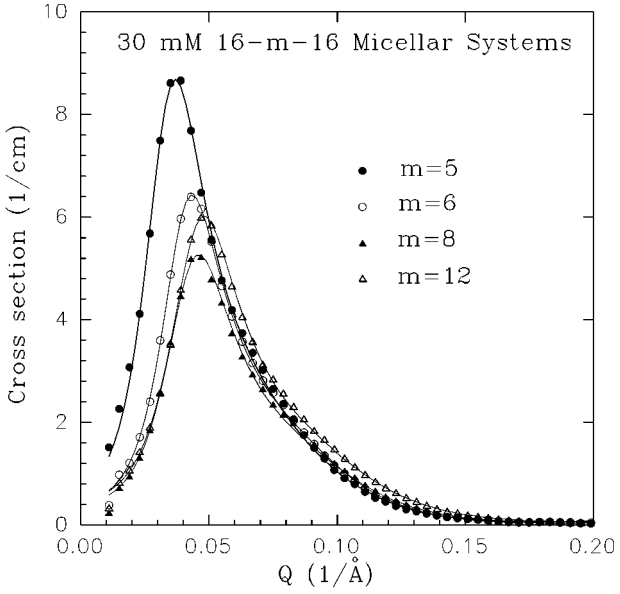

FIG. 6. SANS distributions from 30-mM 16-m-16 ($m \geqslant 5$) micellar systems. Solid lines are theoretical fits of a Hayter-Penfold–type analysis.

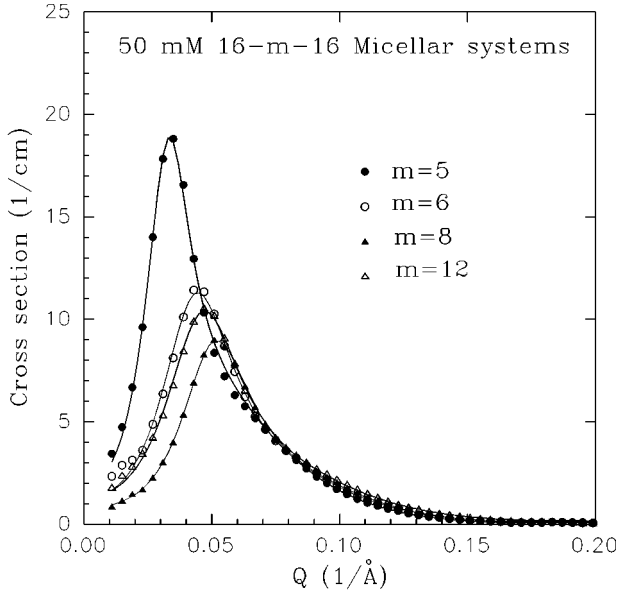

FIG. 7. SANS distributions from 50-mM 16-m-16 ($m \geqslant 5$) micellar systems. Solid lines are theoretical fits of a Hayter-Penfold–type analysis.

micellar structure changes as the concentration increases. The effect is different in the different ranges of the concentration. For example, micellar parameters do not change much as the concentration changes four times from 2.5 to 10 mM (Table II). However, micellar parameters change significantly when the concentration increases from 10 to 50 mM (Table III). The minor axis of the micelle does not change much with the surfactant concentration. It has thus been kept fixed at an average of the values as obtained from the data at the different concentrations. The aggregation number and micellar size increase as the concentration increases. The fractional charge and the effective head group area decrease with the increase in the concentration. These changes are more pronounced for $m=5$ and 12 as compared to those for the intermediate spacer lengths. The fact that the $m=12$ system behaves like a short spacer system is connected to the change of conformation of the spacer.

C. Conformation of spacer and hydrophobic chains in the micelle

The packing parameter p is a useful quantity to determine the micellar structure of surfactant molecules. The parameter is defined in terms of three quantities: (i) volume v, (ii) effective head group area A, and (iii) effective chain length l of the surfactant molecule. It is given as $p=v/Al$. Israelachvili *et al.* have shown that the surfactant molecules with $p<0.33$ tend to form spherical micellar structures. Micelles are ellipsoidal or cylindrical for $0.33 < p < 0.5$. For the higher values of packing parameter $p>0.5$, surfactant molecules aggregate to form disks, membranes, vesicles, etc. In

TABLE III. Micellar structures of 16-m-16 ($m \geqslant 5$) dimeric surfactants at higher concentrations. (a) 16-m-16 ($m \geqslant 5$) micellar systems for $C=30$ mM. The parameters have been obtained by a Hayter-Penfold–type analysis. Micelles are assumed to be prolate ellipsoidal ($b=c \neq a$). (b) 16-m-16 ($m \geqslant 5$) micellar systems for $C=50$ mM. The parameters have been obtained by a Hayter-Penfold–type analysis. Micelles are assumed to be prolate ellipsoidal ($b=c \neq a$).

System	Aggregation number N	Fractional charge α	Minor axis $b=c$ (Å)	Major axis a (Å)	a/b	Effective head group area A (Å^2)
			(a)			
16-5-16	124	0.14	24.2	59.8	2.47	108.5
16-6-16	79	0.27	23.4	41.8	1.78	128.0
16-8-16	66	0.30	22.8	38.6	1.70	141.0
16-12-16	70	0.32	21.8	48.6	2.23	145.0
			(b)			
16-5-16	238	0.11	24.2	115.0	4.75	87.0
16-6-16	108	0.16	23.4	57.5	2.46	116.0
16-8-16	72	0.29	22.8	42.0	1.82	136.0
16-12-16	88	0.19	21.8	60.8	2.79	134.0

TABLE IV. Packing parameter for surfactant molecules in 10-mM 16-*m*-16 micellar systems. v has been calculated from Tanford's formula and A and l are obtained from the analysis.

System	Volume v (Å^3)	Effective head group area A (Å^2)	Effective chain length l (Å)	Packing parameter p
16-3-16	1133	84.0	27.0	0.500
16-4-16	1160	95.5	25.0	0.486
16-5-16	1187	124.5	24.2	0.394
16-6-16	1213	135.0	23.4	0.384
16-8-16	1267	147.0	22.8	0.378
16-10-16	1321	161.0	22.3	0.368
16-12-16	1375	162.0	21.8	0.390

dimeric surfactants, the micellar structure can be easily controlled by changing the spacer length. The change in the spacer length changes the packing parameter and hence the structure.

The values of v, A, l, and p for surfactant molecules in 10-mM 16-*m*-16 micellar solutions are given in Table IV. The volume of surfactant molecule v is obtained using Tanford's formula. The volume of molecule increases by 26.9 Å^3 when one (CH_2) unit is added to the spacer. The effective length l of the molecule is obtained from the data and has been assumed to be the minor axis of the micelle. The effective head group area A is also obtained from the data and is simply the total surface area of the micelle divided by the aggregation number.

It is seen that the effective length of surfactant molecule decreases as the length of the spacer increases. This is connected to the fact that an increase in spacer length results in a gap between the hydrophobic chains, and to fill this gap, the hydrophobic chains fold up in the interior of the micelle. It has also been seen that the effective head group area increases with an increase in the spacer length and becomes constant for long spacers. The effective head group area becoming constant for large spacer length means that the spacer is no longer extended and starts looping inside the micelle. These results suggest that conformation of the spacer and the hydrophobic chains in the micelle changes as the length of the spacer increases. It is of interest to carry out contrast variation experiments with deuterated spacers to explore the conformational changes in the micelle.

The values of packing parameter for $m=3$, 4, 5, 6, 8, 10, and 12 are 0.5, 0.486, 0.394, 0.384, 0.378, 0.368, and 0.39, respectively. They form disk micelles for $m=3$, cylindrical for $m=4$, and prolate ellipsoidal for $m\geqslant 5$. That is, we find that there is a good correspondence between the packing parameter and the experimental structures, in agreement with the theoretical predictions of Israelachvili *et al.*

V. SUMMARY

Micellar structures of bis-cationic 16-*m*-16 dimeric surfactants have been studied using SANS. Measurements were made for different length of hydrocarbon spacers, $m=3$–6, 8, 10, and 12, at various concentrations. It is found that the micellar structure depends on the length of the spacer. Micelles are disks for $m=3$, cylindrical for $m=4$, and prolate ellipsoidals for other values of m. The fractional charge on the micelle increases with an increase in the spacer length. The variation in the length and effective head group area of the surfactant molecules in the micelles shows that the conformation of hydrophobic chains and the spacer change when the length of the spacer increases. The length of the surfactant molecule decreases monotonically with an increase in the length of the spacer. The effective head group area increases as the length of the spacer is increased and becomes constant for long spacers. The concentration dependence for $m\geqslant 5$ shows that the micellar size increases and the fractional charge decreases when the surfactant concentration increases. It is seen that the effect of concentration is more pronounced for $m=5$ and 12. The packing parameter is higher for $m=5$ and 12 than for the intermediate spacers. The long spacer surfactant system behaves like that of a short spacer as there is a tendency of the spacer to loop inside the micelle.

[1] V. Degiorgio and M. Corti, *Physics of Amphiphiles: Micelles, Vesicles and Microemulsions* (North-Holland, Amsterdam, 1985).
[2] Y. Chevalier and T. Zemb, Rep. Prog. Phys. **53**, 279 (1990).
[3] F. M. Menger and C. A. Littau, J. Am. Chem. Soc. **113**, 1451 (1991).
[4] R. Zana, M. Benrraou, and R. Rueff, Langmuir **7**, 1072 (1991).
[5] M. J. Rosen, CHEMITECH **23**, 30 (1993).
[6] R. Zana and Y. Talmon, Nature **362**, 228 (1993).
[7] J. N. Israelachvili, D. J. Mitchell, and B. W. Ninham, J. Chem. Soc., Faraday Trans. II **72**, 1525 (1976).
[8] S. Karaborni, K. Esselink, P. A. J. Hilbers, B. Smit, J. Karthauser, N. M. van Os, and R. Zana, Science **266**, 254 (1994).
[9] D. Danino Y. Talmon, and R. Zana, Langmuir **11**, 1448 (1995).
[10] H. Hirata, N. Hattori, M. Ishida, H. Okabayashi, M. Frusaka, and R. Zana, J. Phys. Chem. **99**, 17 778 (1995).
[11] S. De, V. K. Aswal, P. S. Goyal, and S. Bhattacharya, J. Phys. Chem. **100**, 11 664 (1996).
[12] S. H. Chen, Annu. Rev. Phys. Chem. **37**, 351 (1986).
[13] P. S. Goyal, Phase Transit. **50**, 143 (1994).
[14] S. De, V. K. Aswal, P. S. Goyal, and S. Bhattacharya, J. Phys. Chem. B **101**, 5639 (1997).
[15] P. S. Goyal, V. K. Aswal, and J. V. Joshi, Bhabha Atomic Research Centre Report No. BARC/1995/I/018, 1995.
[16] R. K. Heenan and S. M. King, in *Proceedings of the International Seminar on Structural Investigations at Pulsed Neutron Sources, Dubna*, 1992, edited by V. L. Aksenov, A. M. Balagurov, and Y. V. Taran (JINR, Dubna, 1993).
[17] S. H. Chen and T. L. Lin, *Methods of Experimental Physics* (Academic, New York, 1987), Vol. 23B, p. 489.
[18] C. Tanford, *The Hydrophobic Effect: Formation of Micelles and Biological Membranes* (Wiley, New York, 1980).

[19] A. Guinier and G. Fournet, *Small Angle Scattering of X-Rays* (Wiley, New York, 1955).
[20] J. B. Hayter and J. Penfold, Mol. Phys. **42**, 109 (1981).
[21] J. B. Hayter and J. Penfold, Colloid Polym. Sci. **261**, 1022 (1983).
[22] D. Bendedouch and S. H. Chen, J. Phys. Chem. **88**, 648 (1984).
[23] P. S. Goyal, S. V. G. Menon, B. A. Dasannacharya, and V. Rajagopalan, Chem. Phys. Lett. **211**, 559 (1993).
[24] O. Glatter and O. Kratky, *Small-Angle X-Ray Scattering* (Academic, London, 1982).
[25] C. G. Windsor, J. Appl. Crystallogr. **21**, 582 (1988).
[26] E. Alami, G. Beinert, P. Marie, and R. Zana, Langmuir **9**, 1465 (1993).
[27] S. Bucci, C. Fagotti, V. Degiorgio, and R. Piazza, Langmuir **7**, 824 (1991).
[28] F. Kern, F. Lequeux, R. Zana, and S. J. Candau, Langmuir **10**, 1714 (1994).